Supplemental Data

Genetic Structure and Extinction of the Woolly Mammoth, *Mammuthus primigenius*

Ian Barnes, Beth Shapiro, Adrian Lister, Tatiana Kuznetsova, Andrei Sher, Dale Guthrie, and Mark G. Thomas

Supplemental Experimental Procedures

Primer Sequences

Three different PCR-amplification strategies were employed to generate the 741 bp contig used in this analysis, as discussed in the Experimental Procedures.

Strategy 1

mam_15038F GGCGTCCTAGCCCTACTCCTATCAAT
mam_15399R TTGTTTGCAGGGAATAGTTTAAGAAG
mam_15178F TGAATTGGCAGCCAACCAGTAGAA
mam_15530R TATAAGCATGGGGTAAATAATGTGATG
mam_15393F CCTCGCTATCAATACCCAAAACTG
mam_15780R CGAGAAGAGGGACACGAAGATG

Strategy 2

Like strategy 1, replacing 15393F/15780R with

mam_15528F TAGACCATACCATGTATAATCG
mam_15656R GAGCTTTAATGTGCTATGTAAG
mam_15636F ATGTTTCAGCTCATGGATATTATTC
mam_15780R as above

Strategy 3

mam_15038F as above
mam_15183R AGGCTATTTGGCCGATAATGATGTAG
mam_15175F CATGAATTGGCAGTCAACCAGTAG
mam_15311R TGGCTTTCATTTATGGCTTACAAG
mam_15270F ATTGCAGGAATAATCGAAAACTAC
mam_15401R TGCTTGCAGGGAATAGTTTAAG
mam_15393F as above
mam_15530R as above
mam_15474F ATGCTCGTCCCCATACATAATG
mam_15626R TGGTTTATCGTAGGTGAATAATATC
mam_15574F GCTTATAAGCAAGCACTGTTTAATC
mam_15709R GGAGGTGATATGCATGATGACTAG
mam_15686F AGCACATTAAAGCTCTTGATCGTACA
mam_15780R as above

Supplemental References

S1. Krause, J., Dear, P.H., Pollack, J.L., Slatkin, M., Spriggs, H., Barnes, I., Lister, A.M., Ebersberger, I., Paabo, S., and Hofreiter, M. (2006). Multiplex amplification of the mammoth mitochondrial genome and the evolution of *Elephantidae*. Nature *439*, 742–747.

S2. Rogaev, E.I., Moliaka, Y.K., Malyarchuk, B.A., Kondrashov, F.A., Derenko, M.V., Chumakov, I., and Grigorenko, A.P. (2006). Complete mitochondrial genome and phylogeny of Pleistocene mammoth *Mammuthus primigenius*. PLoS Biol. *4*, e73.

S3. Gilbert, M.T.P., Binladen, J., Miller, W., Wiuf, C., Willerslev, E., Poinar, H., Carlson, J.E., Leebens-Mack, J.H., and Schuster, S.C. (2007). Recharacterization of ancient DNA miscoding lesions: Insights in the era of sequencing-by-synthesis. Nucleic Acids Res. *35*, 1–10.

S4. Poinar, H., Schwarz, C., Qi, J., Shapiro, B., MacPhee, R.D.E., Buigues, B., Tikhonov, A., Huson, D.H., Tomsho, L.P., Auch, A., et al. (2006). Metagenomics to paleogenomics: Large-scale sequencing of mammoth DNA. Science *311*, 392–394.

S5. Guthrie, R.D. (2006). New carbon dates link climatic change with human colonization and Pleistocene extinctions. Nature *441*, 207–209.

S6. Sher, A., Kuzmina, S., Kuznetsova, T., and Sulerzhitsky, L. (2005). New insights into the Weichselian environment and climate of the Eastern-Siberian Arctic, derived from fossil plants, insects and animals. Quat. Sci. Rev. *24*, 533–569.

S7. Guthrie, R.D. (2004). Radiocarbon evidence of mid-Holocene mammoths stranded on an Alaskan Bering Sea island. Nature *249*, 746–749.

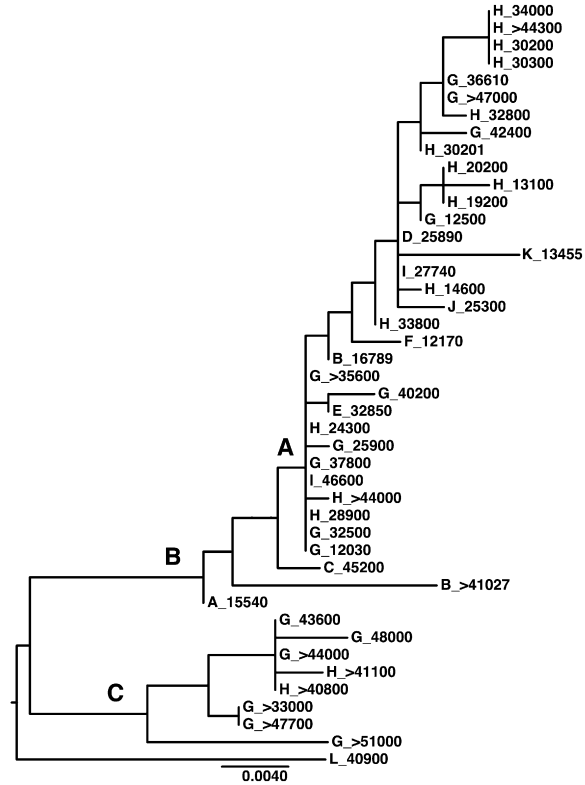

Figure S1. ML Tree as Shown in Figure 2 Describing the Nodes Listed in Table S3

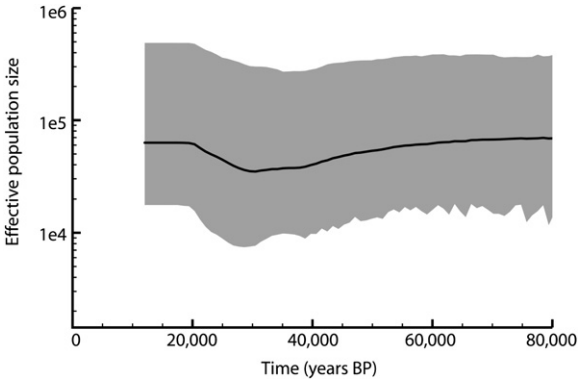

Figure S2. A Bayesian Skyline Plot Showing the Estimated Effective Population Size, N_e, through Time

The black line is the mean value of N_e, and the gray area indicates the 95% highest probability density.

Table S1. Samples Used in This Study

Lab Number	Reference Number	Element	C14 Number	C14 Date	Standard Deviation	Location	Map Reference	Dating Reference	PCR Strategy
TB159	PIN 3751-162	M3	AA 22599	>40800	—	Buor-Khaya Peninsula	H	e	2
TB151	PIN 3751-161	M3	AA 22601	>41100	—	Buor-Khaya Peninsula	H	e	2
TB237	AM 4136	molar fragment	AA14887	>41027	—	Gold Hill	B	a	3
TB164	AM 493	molar fragment	AA14894	15540	145	Ban Creek	A	a	3
TB212	AM 8744	molar fragment	AA14896	16789	100	Ester Creek	B	a	2
TB251	BR.10	tooth	OxA 12058	40900	600	Koosa	L	c	3
TB124	MKh-O447	rib	GIN 10234	14600	100	Bykovsky Peninsula	H	b	1
TB125	MKh-O621	rib	GIN 10235	19200	200	Bykovsky Peninsula	H	b	2
TB128	MKh-O422	scapula fragment	GIN 10236	20200	100	Bykovsky Peninsula	H	b	1
TB130	MKh-O428	scapula	GIN 10237	>44000	—	Bykovsky Peninsula	H	b	2
TB87	MKh-O435	pelvis fragment	GIN 10242	13100	500	Bykovsky Peninsula	H	b	1
TB145	MKh-O437	ulna fragment	GIN 10243	>44300	—	Bykovsky Peninsula	H	b	2
TB89	Mkh-O433	ulna	GIN 10244	30300	600	Bykovsky Peninsula	H	b	1
TB79	MKh-O438	rib	GIN 10245	29400	600	Bykovsky Peninsula	H	b	1
TB75	MKh-O429	pelvis fragment	GIN 10247	28900	200	Bykovsky Peninsula	H	b	1
TB201	MKh-O533	limb bone frag	GIN 10261	34000	500	Bykovsky Peninsula	H	b	2
TB90	MKh-O326	tibia juv frag	GIN 10263	33800	260	Bykovsky Peninsula	H	b	1
TB126	MKh-O381	thoracic vertebra	GIN 10264	24300	200	Bykovsky Peninsula	H	b	2
TB76	MKh-O430	femur fragment	GIN 10266	32800	800	Bykovsky Peninsula	H	b	1
TB78	BL-O865	thoracic vertebra	GIN 10659	32500	500	Bolshoy Lyakhovsky Isl.	G	b	1
TB162	BL-O13	thoracic vertebra	GIN 10660	37800	900	Bolshoy Lyakhovsky Isl.	G	b	2
TB158	BL-O179	lumbar vertebra	GIN 10689	>35600	—	Bolshoy Lyakhovsky Isl.	G	b	2
TB203	BL-O59	fibula fragment	GIN 10697	>42400	—	Bolshoy Lyakhovsky Isl.	G	b	2
TB161	BL-O723	atlas	GIN 10700	>33000	—	Bolshoy Lyakhovsky Isl.	G	b	2
TB77	BL-O585	humerus	GIN 10703	40200	900	Bolshoy Lyakhovsky Isl.	G	b	1
TB157	BL-O503	scapula fragment	GIN 10704	>47700	—	Bolshoy Lyakhovsky Isl.	G	b	2
TB127	BL-O208	pelvis fragment	GIN 10708	25900	600	Bolshoy Lyakhovsky Isl.	G	b	1
TB129	BL-O443	tusk frag	GIN 10709	48000	2000	Bolshoy Lyakhovsky Isl.	G	b	2
TB92	BL-O240	tusk frag	GIN 10710	>51000	—	Bolshoy Lyakhovsky Isl.	G	b	1
TB93	BL-O310	pelvis	GIN 10711	>44000	—	Bolshoy Lyakhovsky Isl.	G	b	1
TB147	BL-O309	femur fragment	GIN 10712	>47000	—	Bolshoy Lyakhovsky Isl.	G	b	2
TB80	BL-O250	ulna fragment	GIN 10713	12030	60	Bolshoy Lyakhovsky Isl.	G	b	1
TB123	BL-O219	tusk fragment	GIN 10716	12500	500	Bolshoy Lyakhovsky Isl.	G	b	1
TB94	BL-O308	scapula fragment	GIN 10717	43600	1000	Bolshoy Lyakhovsky Isl.	G	b	1
TB95	Nag-99-O203	cranium	GIN 10719	30200	400	Lena Delta Region	H	b	1
TB242	ILC.01(10915)	ivory	OxA 11813	45200	800	Kamchatka	C	c	2
TB181	ILC.04(11028)	ivory	OxA 11748	36610	360	Bolshoy Lyakhovsky Isl.	G	c	2
TB182	ILC.06(1138a)	tooth	OxA 11839	46600	1100	Khatanga River Mouth	I	c	2
TB188	ILC.08(10643)	bone	OxA 11841	25890	140	Wrangel Island	D	c	2
TB245	WS.02	bone	OxA 12030	13455	60	Lugovskoe	K	c	2
TB185	WS.04	ivory	OxA 12032	25300	290	Kochegur	J	c	2
Ref. [S1]		bone	KIA 25289	12170	50	Berelyokh	F		
Ref. [S2]		frozen leg skin	MAG 1001	32850	900	Enmynveem	E		
Refs. [S3, S4]		mandible	Beta 210777	27740	220	Taimyr Lake	I		

Sampling locations are as in Figure 1 in the main text. In the Dating Reference column, "a" denotes sampled by D.G. [S5], "b" denotes collected by T.K [S6], "c" denotes sampled by A.J. Stuart and A.L., and "e" denotes sampled by A.S.

Table S2. Samples for which DNA Amplifications Were Not Successful

Lab Number	Reference Number	Element	C14 Number	C14 Date	Standard Deviation	Location	Map Reference	Dating Reference
TB215	166	tooth	AA 14855	26022	640	Cripple Cr.	B	a
TB208	167	tooth	AA 14856	39151	3232	Fairbanks Cr.	B	a
TB218	168	tooth	AA 14857	>41086	—	Cripple Cr.	B	a
TB243	169	tooth	AA 14858	>41094	—	Cripple Creek	B	a
TB232	173	tooth	AA 14862	>41063	—	Cleary Cr.	B	a
TB229	175	tooth	AA 14864	23222	453	Goldstream	B	a
TB224	176	tooth	AA 14865	>41096	—	Engineer Cr.	B	a
TB233	177	tooth	AA 14866	16168	209	Cleary Cr.	B	a
TB222	179	tooth	AA 14868	23015	449	Goldstream	B	a
TB231	180	tooth	AA 14869	37331	2516	Ester Cr	B	a
TB213	181	tooth	AA 14870	25362	584	Cleary Cr.	B	a
TB217	182	tooth	AA 14871	>41064	—	Cripple Cr.	B	a
TB206	185	tooth	AA 14874	40515	3850	Engineer Cr.	B	a
TB220	186	tooth	AA 14875	>40925	—	Ester Cr.	B	a
TB223	187	tooth	AA 14876	35700	2155	Goldstream	B	a
TB214	188	tooth	AA 14877	>41037	—	Engineer Cr.	B	a
TB236	190	tooth	AA 14879	>41096	—	Goldstream	B	a
TB211	191	tooth	AA 14880	12576	147	Goldstream	B	a
TB209	192	tooth	AA 14881	23808	487	Gilmore Cr.	B	a
TB235	193	tooth	AA 14882	14679	174	Ban Cr.	B	a
TB226	194	tooth	AA 14883	13410	152	Ester Cr.	B	a
TB221	195	tooth	AA 14884	>41007	—	Fairbanks area	B	a
TB225	203	tooth	AA 14892	14093	163	Cleary Cr.	B	a
TB207	204	tooth	AA 14893	47116	2854	Engineer Cr.	B	a
TB230	206	tooth	AA 14895	14023	98	Fairbanks Cr.	B	a
TB219	207	tooth	AA 14362	37359	2532	Inglutalik Cr.	B	a
TB210	208	tooth	AA 14363	31360	1251	Inglutalik Cr.	B	a
TB205	210	tooth	AA 14365	>41081	—	Inglutalik Cr.	B	a
TB227	210	tooth	AA 14365	>41081	—	Inglutalik Cr.	B	a
TB184	2815-2	bone	OxA 11292	23940	180	Third Cave	*Europe*	c
TB163	761-51	mandible	N/A		—	Alyoshkina	*Europe*	c
TB190	BR.10	tooth	OxA 12058	40900	600	Koosa	*Europe*	c
TB247	BR.10	tooth	OxA 11410	30100	270	Hornsea	*Europe*	c
TB248	BS.12	ivory	OxA 11562	34810	340	Tudulinna2	*Europe*	c
TB249	BS.13	ivory	OxA 11563	46500	1000	Ihasalu	*Europe*	c
TB250	BS.15	tooth	OxA 11607	28780	160	Valga	*Europe*	c
TB155	BL-O260	fibula fragment	GIN 10705	>42000	—	Bolshoy Lyakhovsky Isl.	G	b
TB74	BL-O444	scapula	GIN 10239	14500	110	Bolshoy Lyakhovsky Isl.	G	b
TB121	BL-O508	pelvis fragment	GIN 10707	22100	1000	Bolshoy Lyakhovsky Isl.	G	b
TB187	ILC.02(11315)	bone	OxA 11746	23560	140	Pogon	*Europe*	c
TB196	ILC.03(10884)	bone	OxA 11747	30420	250	Sungir	*Europe*	c
TB197	ILC.05(11200)	bone	OxA 11974	13945	50	Obukhov Town	*Europe*	c
TB194	ILC.07(10716)	ivory	OxA 11840	13180	60	Bolshoy Lyakhovsky Isl.	G	c
TB244	ILC.09(10908)	ivory	OxA 11842	17740	90	Mama River	*E. Siberia*	c
TB193	IT.36	bone	OxA 11283	39650	700	Acqualunga	*Europe*	c
TB198	Po.19	bone	OxA 11058	44100	1200	Szczecin	*Europe*	c
TB246	SwZ.01	ivory	OxA 12982	13705	55	Praz Rodet	*Europe*	c
TB152	USNM 23455	tooth	OxA 13027	8010	40	Pribiloff Island	*Bering Strait*	d
TB191	WE.03	bone	OxA 12018	12235	75	Buisson Campin	*Europe*	c
TB186	WE.04A	bone	OxA 12019	12315	55	Etoilles	*Europe*	c
TB195	WE.05	tooth	OxA 12020	12800	65	Marolles-sur-Seine	*Europe*	c
TB189	WS.01	bone	OxA 12029	13450	50	Lugovskoe	K	c
TB183	WS.03	tooth	OxA 12031	13205	60	Lugovskoe	K	c

Sampling locations are as in Figure 1 in the main text. In the Dating Reference column, "a" denotes sampled by D.G. [S5], "b" denotes collected by T.K [S6], "c" denotes sampled by A.J. Stuart and A.L., and "d" denotes sampled by D.G. [S7].

Table S3. Results of 12 BEAST Analyses with 33 Mammoth Sequences with Finite Radiocarbon Dates

A. Strict-Clock, Relaxed Demographic Model

	Mean (ln) posterior (HKY+G)	Mean (ln) posterior (HKY+I)	Rate (HKY+G)	Rate (HKY+I)	Node A (HKY+G)	Node A (HKY+I)	Node B (HKY+G)	Node B (HKY+I)	Node C (HKY+G)	Node C (HKY+I)
Mean	−1885.723	−1848.622	1.21E-07	1.91E-07	8.69E+04	6.38E+04	1.23E+05	6.84E+04	2.62E+05	1.67E+05
95% HPD lower			6.66E-09	6.62E-08	4.68E+04	4.68E+04	4.90E+04	4.96E+04	7.49E+06	8.42E+04
95% HPD upper			2.44E-07	3.15E-07	1.72E+05	8.68E+04	2.65E+05	9.50E+04	5.78E+05	2.88E+05
Effective sample size			349.893	912.876	438.983	729.567	433.028	671.67	433.571	741.605

B. Relaxed-Clock, Relaxed Demographic Model

	Mean (ln) posterior (HKY+G)	Mean (ln) posterior (HKY+I)	Rate (HKY+G)	Mean Rate (HKY+I)	Node A (HKY+G)	Node A (HKY+I)	Node B (HKY+G)	Node B (HKY+I)	Node C (HKY+G)	Node C (HKY+I)
Mean	−1855.16	−1823.157	1.30E-07	2.47E-07	7.79E+04	6.34E+04	1.19E+05	6.92E+04	2.00E+05	1.48E+05
95% HPD lower			2.31E-08	6.32E-08	4.66E+04	4.66E+04	4.86E+04	4.72E+04	6.22E+04	5.18E+05
95% HPD upper			2.61E-07	4.53E-07	1.39E+05	9.40E+04	2.44E+05	1.07E+05	4.30E+05	2.85E+05
Effective sample size			699.342	1457.547	1.31E+04	1.50E+04	1.33E+04	1.40E+04	1.34E+04	1.46E+04

C. Strict-Clock, Constant-Population-Size Demographic Model

	Mean (ln) posterior (HKY+G)	Mean (ln) posterior (HKY+I)	Rate (HKY+G)	Rate (HKY+I)	Node A (HKY+G)	Node A (HKY+I)	Node B (HKY+G)	Node B (HKY+I)	Node C (HKY+G)	Node C (HKY+I)
Mean	−1821.807	−1800.81	8.64E-08	1.27E-07	102930	88890	152030	98030	345130	295430
95% HPD lower			4.43E-09	3.23E-08	48690	48190	52270	50500	98480	90540
95% HPD upper			1.64E-07	2.51E-07	204930	145230	329930	162230	772130	550530
Effective sample size			556.439	677.574	348.428	221.773	346.352	237.309	384.345	232.843

D. Relaxed-Clock, Constant-Population-Size Demographic Model

	Mean (ln) posterior (HKY+G)	Mean (ln) posterior (HKY+I)	Rate (HKY+G)	Mean Rate (HKY+I)	Node A (HKY+G)	Node A (HKY+I)	Node B (HKY+G)	Node B (HKY+I)	Node C (HKY+G)	Node C (HKY+I)
Mean	−1806.263	−1785.917	9.54E-08	1.64E-07	106150	78230	170730	94500	330830	224130
95% HPD lower			6.01E-09	2.32E-08	47250	46830	52430	47860	75020	62900
95% HPD upper			1.84E-07	3.38E-07	210630	134630	387930	185130	778530	466030
Effective sample size			436.788	468.906	606.36	625.128	420.157	541.558	383.707	644.938

E. Strict-Clock, Exponential-Growth Demographic model

	Mean (ln) posterior (HKY+G)	Mean (ln) posterior (HKY+I)	Rate (HKY+G)	Rate (HKY+I)	Node A (HKY+G)	Node A (HKY+I)	Node B (HKY+G)	Node B (HKY+I)	Node C (HKY+G)	Node C (HKY+I)
Mean	−1818.972	−1795.462	9.64E-08	1.46E-07	88090	73570	123330	80710	251730	212630
95% HPD lower			1.54E-08	3.77E-08	49250	47530	52650	49860	92300	88770
95% HPD upper			1.76E-07	2.59E-07	157230	111740	237630	125630	501030	385930
Effective sample size			702.622	728.623	570.783	501.525	568.891	486.281	609.051	534.064

F. Relaxed-Clock, Exponential-Growth Demographic Model

	Mean (ln) posterior (HKY+G)	Mean (ln) posterior (HKY+I)	Rate (HKY+G)	Mean Rate (HKY+I)	Node A (HKY+G)	Node A (HKY+I)	Node B (HKY+G)	Node B (HKY+I)	Node C (HKY+G)	Node C (HKY+I)
Mean	−1800.88	−1772.466	1.28E-07	2.72E-07	97150	67280	122230	72990	153130	104960
95% HPD lower			1.29E-08	2.91E-08	46630	46600	49480	46600	52700	48110
95% HPD upper			2.43E-07	5.55E-07	217230	114930	275430	131830	362230	228030
Effective sample size			223.205	269.597	163.711	256.014	170.94	205.103	228.84	386.831

The best-fitting strict- and relaxed-clock models are indicated by underlining.